European Journal of Medicinal Chemistry 250 (2023) 115169

Contents lists available at ScienceDirect

European Journal of Medicinal Chemistry

journal homepage: www.elsevier.com/locate/ejmech

Research paper

Thioxanthenone-based derivatives as multitarget therapeutic leads for Alzheimer's disease

Michele Tonelli [a,*], Marco Catto [b,**], Raimon Sabaté [c,***], Valeria Francesconi [a], Erik Laurini [d], Sabrina Pricl [d,e], Leonardo Pisani [b], Daniela Valeria Miniero [f], Grazia Maria Liuzzi [f], Elena Gatta [g], Annalisa Relini [g], Rosalina Gavín [h,i,j], Jose Antonio Del Rio [h,i,j], Fabio Sparatore [a], Angelo Carotti [b]

[a] Department of Pharmacy, University of Genoa, 16132, Genoa, Italy
[b] Department of Pharmacy-Pharmaceutical Sciences, University of Bari Aldo Moro, 70125, Bari, Italy
[c] Department of Pharmacy and Pharmaceutical Technology and Physical-Chemistry, Faculty of Pharmacy and Food Sciences, and Institute of Nanoscience and Nanotechnology (IN2UB), University of Barcelona, 08028, Barcelona, Spain
[d] Molecular Biology and Nanotechnology Laboratory (MolBNL@UniTS), Department of Engineering and Architecture, University of Trieste, 34127, Trieste, Italy
[e] Department of General Biophysics, Faculty of Biology and Environmental Protection, University of Lodz, 90-236, Lodz, Poland
[f] Department of Biosciences, Biotechnologies and Environment, University of Bari Aldo Moro, 70125, Bari, Italy
[g] Department of Physics, University of Genoa, 16146, Genoa, Italy
[h] Institute for Bioengineering of Catalonia (IBEC), The Barcelona Institute of Science and Technology, 08028, Barcelona, Spain
[i] Department of Cell Biology, Physiology and Immunology, Faculty of Biology, University of Barcelona, 08028, Barcelona, Spain
[j] Institute of Neuroscience, University of Barcelona, 08028, Barcelona, Spain

ARTICLE INFO

Keywords:
Thioxanthene-9-one and xanthen-9-one derivatives
Alzheimer's disease
Multitarget-directed ligands (MTDLs)
Aβ and tau aggregation inhibition
AChE and BChE inhibition

ABSTRACT

A set of twenty-five thioxanthene-9-one and xanthene-9-one derivatives, that were previously shown to inhibit cholinesterases (ChEs) and amyloid β ($A\beta_{40}$) aggregation, were evaluated for the inhibition of tau protein aggregation. All compounds exhibited a good activity, and eight of them (**5**–**8**, **10**, **14**, **15** and **20**) shared comparable low micromolar inhibitory potency versus $A\beta_{40}$ aggregation and human acetylcholinesterase (AChE), while inhibiting human butyrylcholinesterase (BChE) even at submicromolar concentration. Compound **20** showed outstanding biological data, inhibiting tau protein and $A\beta_{40}$ aggregation with IC_{50} = 1.8 and 1.3 μM, respectively. Moreover, at 0.1–10 μM it also exhibited neuroprotective activity against tau toxicity induced by okadoic acid in human neuroblastoma SH-SY5Y cells, that was comparable to that of estradiol and PD38. In preliminary toxicity studies, these interesting results for compound **20** are somewhat conflicting with a narrow safety window. However, compound **10**, although endowed with a little lower potency for tau and Aβ aggregation inhibition additionally demonstrated good inhibition of ChEs and rather low cytotoxicity. Compound **4** is also worth of note for its high potency as *h*BChE inhibitor (IC_{50} = 7 nM) and for the three order of magnitude selectivity *versus* *h*AChE. Molecular modelling studies were performed to explain the different behavior of compounds **4** and **20** towards *h*BChE.

The observed balance of the inhibitory potencies versus the relevant targets indicates the thioxanthene-9-one derivatives as potential MTDLs for AD therapy, provided that the safety window will be improved by further structural variations, currently under investigation.

1. Introduction

Alzheimer's disease (AD) is an age-related neurodegenerative disorder accounted as the third most frequent human pathology after cancer and cardiovascular diseases. AD is characterized by progressive memory loss and cognitive impairment, leading to dementia and daily

* Corresponding author.
** Corresponding author.
*** Corresponding author.
E-mail addresses: michele.tonelli@unige.it (M. Tonelli), marco.catto@uniba.it (M. Catto), rsabate@ub.edu (R. Sabaté).

https://doi.org/10.1016/j.ejmech.2023.115169
Received 1 January 2023; Received in revised form 27 January 2023; Accepted 28 January 2023
Available online 2 February 2023
0223-5234/© 2023 The Authors. Published by Elsevier Masson SAS. This is an open access article under the CC BY license (http://creativecommons.org/licenses/by/4.0/).

life disability. The histopathological evidence of AD is mainly related to *extracellular* protein aggregates formed by amyloid β (Aβ) peptide (amyloid plaques) and *intracellular* protein deposits constituted by hyperphosphorylated tau protein (neurofibrillary tangles). However, several other pathological factors may contribute to the progression and worsening of AD such as oxidative stress, inflammation, autophagy, mitochondrial disfunctions and so forth [1–3].

The deposition of amyloid plaques, starting from the cholinergic neurons of hippocampus, progressively extends to the whole brain cortex with the loss of cholinergic neurons and the consequent lowering of the synaptic level of neurotransmitter acetylcholine (ACh) [4]. Thus, the current symptomatic therapy of AD mainly relies on the restoration of normal ACh levels [5] through the inhibition of acetyl- and butyrylcholinesterase (AChE and BChE), without provisioning alteration in the disease's prognosis. Interestingly, some cholinesterase inhibitors, namely dual binding site (DBS) inhibitors, besides increasing the ACh levels, may block the aggregation of Aβ promoted by their binding at the enzyme peripheral anionic site (PAS) [6–8].

Aβ aggregation blockade may be provided by different kinds of molecules, most of which have failed in all clinical trials performed so far. However, quite recently, aducanumab, a human monoclonal antibody (MAB) targeting Aβ oligomers, has been approved by the FDA as the first Aβ-directed drug for the therapy of AD [9] even though after many controversies. In addition, preliminary data on lecanemab, another human MAB in clinical trial, showed a significant slow of mental decline in AD patients [10].

It has been argued that soluble low-molecular-weight oligomers, as intermediate species in the aggregation process of Aβ, may be responsible for neuronal damage and ultimately cell death [11]. It has been postulated that Aβ aggregation occurs at early stage of AD, while tau aggregation correlates better to disease progression. Indeed, tau protein displays multiple physiological functions by interacting with a variety of cellular partners, but it is also able to interact with other tau molecules to form oligomers and filaments. The smaller diffusible Aβ oligomers may penetrate cells and trigger tau phosphorylation (and consequent aggregation) and/or direct tau aggregation [12,13]. It has also been suggested [14] a toxic role for extracellular tau (released physiologically, or resulting from the disruption of dead cells), which may spread in the brain, in a prion-like manner [15], as conformationally misfolded monomers, paired helical filaments (PHFs) or other forms, seeding the intracellular aggregation and representing a primary event in AD, even preceding Aβ aggregation.

In addition to the *anti*-Aβ aggregation, the tau aggregation inhibition can be seen as promising disease-modifying treatment (DMT) in AD. With this aim, the prevention of tau aggregation may be gained by dampening its phosphorylation (through the block of specific kinases, or the activation of specific phosphatases), or by the direct inhibition of the initial step of aggregation process. The neuronal uptake of the different kinds of tau aggregates and/or their enhanced clearance, might result even more beneficial for AD therapy.

In order to find Aβ and/or tau aggregation inhibitors, a wide chemical space has been explored, and a huge number of compounds have been illustrated in some reviews and recent articles [13,16–26]. Besides the multiple conjugated double bonds, allowing an extensive delocalization of a cationic charge (as found in cyanines, methylene blue and analogues, presently in a clinical phase III for AD therapy), frequently encountered structural features of aggregation inhibitors are carbonyl groups (isolated or conjugated with a C═C or C═N double bond), in open chain molecules or embodied in mono- or polycyclic systems, commonly further decorated with hydroxy and/or amino groups. Aromatic ketones may also contribute as hydrogen bond acceptor molecules in disrupting the β-sheet ordered sequences responsible for Aβ aggregation [27]. The isolated or conjugated carbonyl functions may undergo imine formation, by reacting with the ε-amino group of lysine residues or by Michael addition reaction with the thiol group of cysteines from tau, respectively. When phenolic hydroxyls are present, while acting as scavenger of oxidative species, they may generate novel carbonyl groups as additional electrophilic centers [28–30]. Examples of these compounds (dyes, chalconoids, flavonoids, quinones and complex polyheterocyclic systems) are depicted in Fig. 1, along with corresponding references [26,31–45].

A few years ago [46], we described sets of carbonyl-containing compounds as naphthoquinone, anthraquinone, xanthene-9-one and thioxanthene-9-one derivatives, acting as multitarget directed ligands (MTDLs) by inhibiting cholinesterases and Aβ aggregation (Fig. 2). These compounds are characterized by the presence of basic side chains, mainly quinolizidinylalkyl moieties, that were previously shown to produce potent cholinesterase inhibition when linked to diverse bi- and tricyclic (hetero)aromatic systems [47].

Most of these compounds exhibited IC_{50} values from the low to submicromolar range *versus* the cited biological targets. The inhibition of Aβ aggregation did not linearly correlate with the inhibition of cholinesterases; nevertheless, some compounds inhibited one or both ChEs and Aβ aggregation with similar potencies, thus fulfilling a fundamental requirement of a multitarget drug, that is balanced pharmacological activities. Moreover, exploratory investigation on a couple of representative compounds [46] indicated that they may cross the BBB with a permeability comparable or even superior to that of diazepam.

Structure-activity correlation suggested that tricyclic compounds are more prone than the bicyclic ones to the inhibition of Aβ aggregation, and among the former, thioxanthenone derivatives emerged as more active inhibitors of Aβ aggregation than xanthenone and anthraquinone derivatives. Moreover, compounds bearing the bulky and highly lipophilic quinolizidine moiety performed better in the inhibition of Aβ aggregation with respect to analogues bearing dialkylaminoalkyl basic chains.

It was additionally observed that the aforementioned thioxanthenone derivatives displayed a high inhibitory activity (IC_{50} range = 0.088–6.1 μM) *versus* butyrylcholinesterase (BChE), that is another designated target in AD due to its compensation character to hydrolyze ACh in progressed disease, and its close relation to progressive Aβ deposition [48]. More recently, the target combination, consisting of the Aβ and tau, has been proposed as the right choice to tackle AD, their aggregation inhibition possessing the potential to deliver DMT effects [13]. Given the multifactorial nature of the onset and development of AD, the MTDL strategy continues to represent a more promising approach than the traditional "one drug-one target" one, even because it could be used in various target combination strategies [49].

2. Results and discussion

In this complex and challenging context, the multitarget profile displayed by the aforementioned thioxanthenone (**1**–**22**) and xanthenone derivatives (**23**–**25**) towards *ee*AChE, *es*BChE, and $Aβ_{40}$ self-aggregation inhibition prompted us to deepen and enlarge the study of their multitarget behavior. Piperidine derivative **20** was designed and prepared with the aim of replacing the quinolizidine basic moiety with the smaller and less lipophilic piperidine but still endowed with greater bulkiness than linear dialkylamine-*O*-alkyl chains. Our aims were the evaluation of the role of the quinolizidine moiety in the diverse inhibition processes, the increasing of aqueous solubility, the decrease of lipophilicity and the reduction of the potential cytotoxicity of our molecules (see section 2.6).

Due to the crosstalk between Aβ and tau leading to AD pathological burden, we assessed the ability of our library to also inhibit tau protein aggregation, as a novel and additional biological property with higher credentials for displaying DMT effects. Accordingly, we first explored the inhibition activity of some representative compounds *versus* faster PHF6 peptide aggregation [50,51], and then, following the positive feedback, we screened the library in a cell-based assay against full-length tau [52]. Finally, to further corroborate their potential therapeutic efficacy, we also evaluated the activity of the most potent

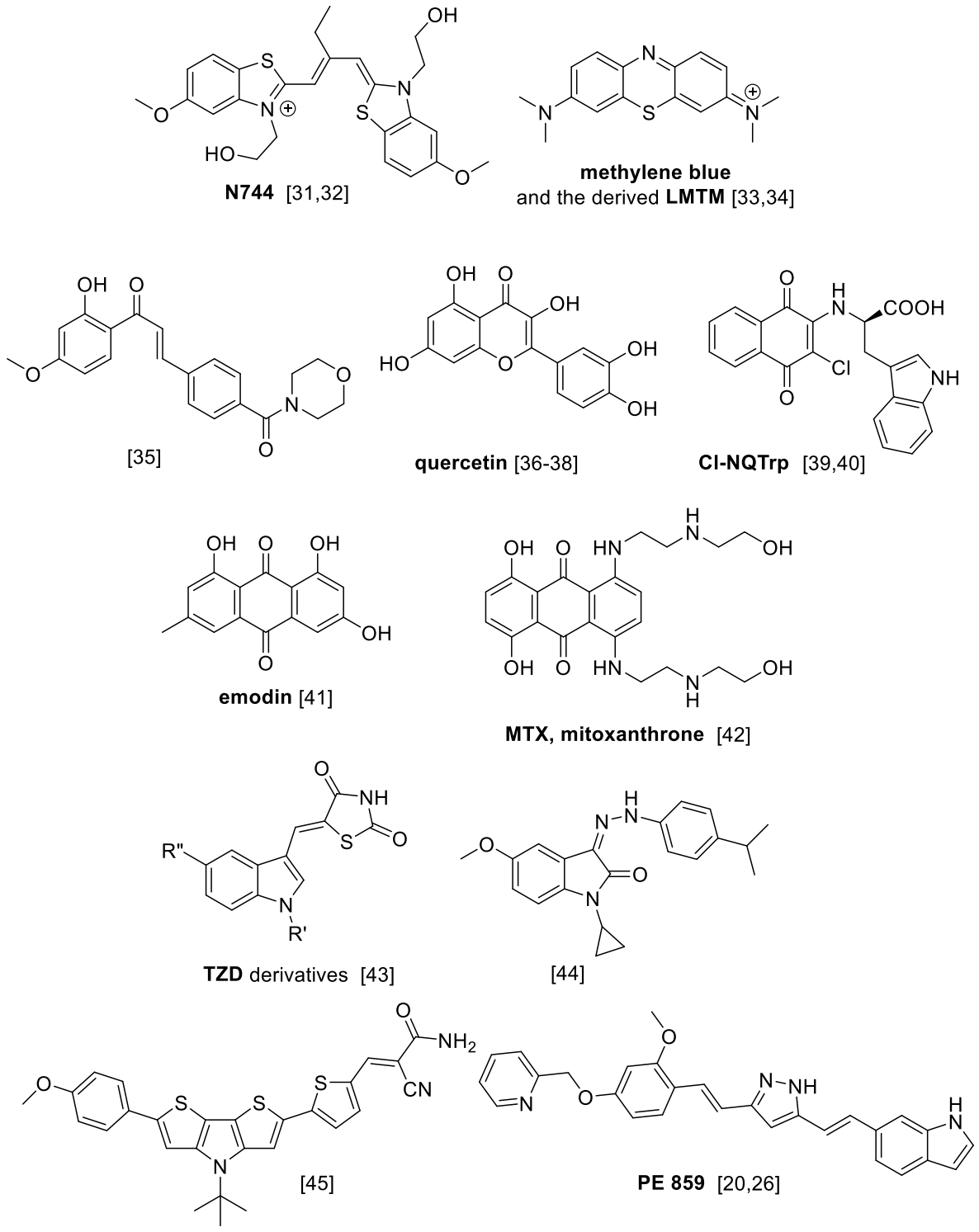

Fig. 1. Examples of Aβ and tau protein aggregation inhibitors (and corresponding references).

ChEs inhibitors against the corresponding human ChEs enzymes.

2.1. Chemistry

The chemical structures of the investigated compounds (22 thioxanthenone and 3 xanthenone derivatives) are depicted in Table 1. With the exception of compound **20**, all compounds of Table 1 were obtained from our in-house library, having been synthesized and studied in the past as antimicrobial, antileishmanial, antileukemia P388 agents [53–55], and as dual inhibitors of ChEs and Aβ aggregation [46]. In particular, the multitarget activities of compounds **1**–**3**, **5**–**12**, **16** and **17** [54], and **4**, **13**–**15**, **18** and **21**–**25** [46] have been described in the quoted references. Compound **19** (lucanthone) was synthesized as reported by Archer and Suter [56]. The newly designed compound **20** was prepared (Scheme 1) by reacting the 2-(1-methylpiperidin-4-yl) ethan-1-amine with 1-chloro-7-methoxy-4-methylthioxanthen-9-one, obtained according to Archer et al. [57].

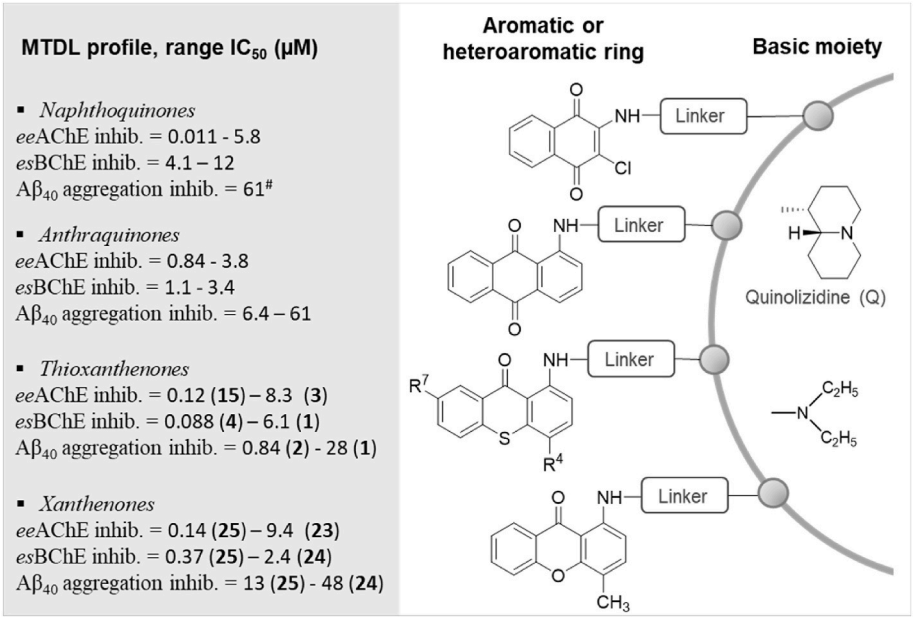

Fig. 2. Schematic representation of our previously studied MTDL [46], efficiently targeting electric eel AChE (*ee*AChE), equine serum BChE (*es*BChE) and $A\beta_{40}$ aggregation; the bold numbers refer to compounds cited also in the present paper. # The IC_{50} value refers to 3-Chloro-2-{[(1*S*,9*aR*)-(octahydro-2H-quinolizin-1-yl) methylthio]-prop-1-ylamino}-1,4-naphthoquinone.

Table 1
Inhibitory activities of thioxanthenone (**1**–**22**) and xanthenone (**23**–**25**) derivatives against tau and Aβ protein aggregation.

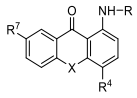	X	R[b]	R^4	R^7	tau aggregation		$A\beta_{40}$ aggregation[a]
					% inhib. at 10 μM	IC_{50} (μM)[c]	IC_{50} (μM)
1	S	CH_2-Q	CH_3	H	nt	nt	28
2	S	CH_2CH_2-Q	CH_3	H		46	0.84
3	S	$CH_2CH_2CH_2$-Q	CH_3	H	26 ± 2		4.3
4	S	$CH_2CH_2CH_2SCH_2$-Q	CH_3	H		20	4.3
5	S	CH_2-Q	CH_3	OH		9.1	5.9
6	S	CH_2CH_2-Q	CH_3	OH		8.9	2.4 ± 0.1
7	S	$CH_2CH_2CH_2$-Q	CH_3	OH		7.3	2.9
8	S	CH_2-Q	CH_3	OCH_3		5.5	4.3
9	S	CH_2CH_2-Q	CH_3	OCH_3		14	2.4 ± 0.1
10	S	$CH_2CH_2CH_2$-Q	CH_3	OCH_3		5.9	2.5
11	S	CH_2-Q	NO_2	H		15	20
12	S	$CH_2CH_2CH_2$-Q	NO_2	H	22 ± 2		13
13	S	CH_2-Q	NO_2	OCH_3	32 ± 2		11
14	S	CH_2CH_2-Q	NO_2	OCH_3		6.9	9.1
15	S	$CH_2CH_2CH_2$-Q	NO_2	OCH_3		3.0	7.9
16	S	CH_2-Q	NH_2	H		8.6	14
17	S	$CH_2CH_2CH_2$-Q	NH_2	H	26 ± 1		1.3
18	S	CH_2CH_2-Q	NH_2	OCH_3	33 ± 2		13
19	S	CH_2CH_2–$N(CH_2CH_3)_2$	CH_3	H		10.9	24
20	S	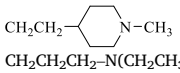	CH_3	OCH_3		1.8	1.3 ± 0.1
21	S	$CH_2CH_2CH_2$–$N(CH_2CH_3)_2$	NO_2	OCH_3		4.8	17
22	S	$CH_2CH_2CH_2$–$N(CH_2CH_3)_2$	NH_2	OCH_3	24 ± 2		21
23	O	$CH_2CH_2CH_2$–$N(CH_2CH_3)_2$	CH_3	H		16	(55)[d]
24	O	CH_2-Q	CH_3	H	35 ± 3		48
25	O	$CH_2CH_2CH_2$-Q	CH_3	H		23	13
Quercetin							0.82 ± 0.07

[a] Values are taken from Ref. [46], except for **6**, **9** and **20**.
[b] Q = quinolizidin-1α-yl moiety.
[c] Values are the mean of three independent experiments, SEM < 10%; nt: not tested.
[d] % inhibition at 100 μM.

2.2. Inhibition of PHF6 and tau aggregation

According to a fast assay based on thioflavin T (ThT) fluorescence [58], six compounds were exploratively tested using the highly repeated peptide sequence (306)VQIVYK(311) of tau responsible for protein aggregation in paired helical fragments (PHF6) [59]. Results depicted in Fig. 3 enlighten the high potency profile of some of the selected compounds in inhibiting PHF6 aggregation, with inhibition >80% at 10 μM concentration for three derivatives **2**, **7** and **22**, comparable to reference compound quercetin. However, while compound **7** was also a good

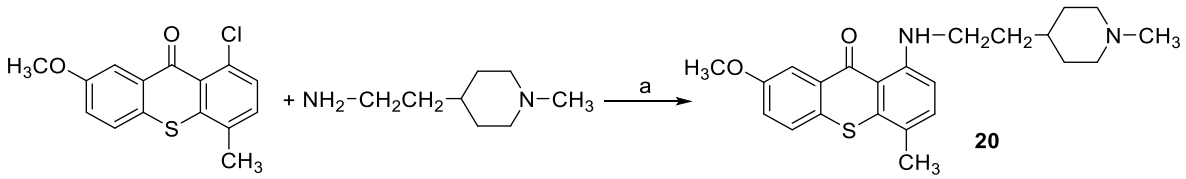

Scheme 1. Reagents and conditions: a) chlorothioxanthenone/amine ratio 1:2, fusion at 170 °C, 6 h.

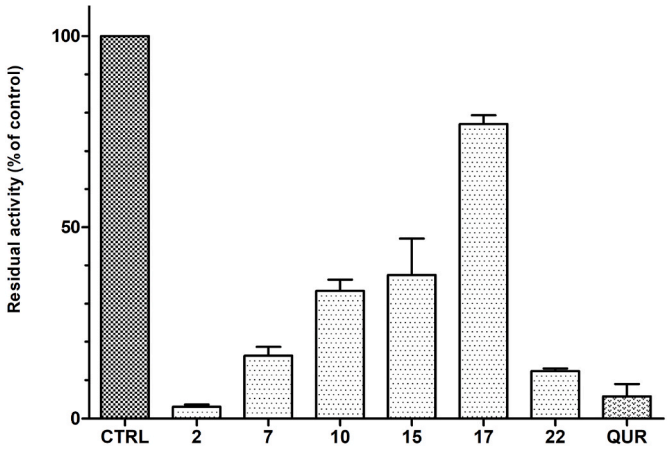

Fig. 3. Inhibition of 50 μM PHF6 aggregation by 10 μM test compounds (ThT fluorescence test); reference quercetin (QUR).

inhibitor of tau aggregation in cellular assay (IC_{50} = 7.3 μM), the other two (**2** and **22**) were less effective (IC_{50} = 46 μM and 24% inhibition at 10 μM), as reported in Table 1. Thus, the aggregation inhibition of tau protein and hexapeptide PHF6 may develop through different modalities in relation to their diverse chemical structures, which may entail distinct binding modes. This trend has also been delineated for other classes of tau aggregation inhibitors [13].

Concerning the full-length tau protein aggregation [52,60], all tested compounds showed an interesting and quite valuable inhibitory activity, with IC_{50} values < 10 μM for the ten most active compounds (**5**–**8**, **10**, **14**–**16**, **20** and **21**). Seven other compounds displayed IC_{50} values in the range 10.9–46 μM, whilst for the remaining ones the IC_{50} could not be assessed because of solubility problems (22–35% inhibition at 10 μM concentration).

Most of the tested compounds inhibited the aggregation of tau protein and $Aβ_{40}$ [46] with similar potencies, suggesting the existence of common epitopes in the two biomolecules [61]. In particular, eight compounds (**5**–**8**, **10**, **14**, **15** and **20**) exhibited IC_{50} < 10 μM *versus* both biomolecules, and compound **20** displayed an outstanding activity, IC_{50} = 1.3 μM and 1.8 μM *versus* Aβ and tau aggregation, respectively. Seven other compounds (**4**, **9**, **11**, **16**, **19**, **21** and **25**), even if endowed with somewhat more divergent potencies *versus* the two targets, may be still considered interesting dual inhibitors of Aβ and tau aggregation. Rather intriguing were the results concerning compounds **2** and **17**, which, while displaying high potencies against Aβ aggregation (IC_{50} = 0.84 μM and 1.3 μM, respectively), exhibited modest or poor inhibitory activity *versus* tau aggregation (IC_{50} = 46 μM and 26% inhibition at 10 μM concentration).

Each considered structural feature (nature and length of the linker chain, nature of substituents in positions 4 and 7 of tricyclic system) may be associated with some degree of inhibition of tau protein aggregation. However, the presence of a substituent (OH or OCH_3) at position 7 warranted a higher activity: ten compounds with IC_{50} in the range 1.8–13.6 μM (mean $IC_{50=}$ 6.7 μM) *versus* seven 7-unsubstituted compounds with IC_{50} in the range 8.6–46 μM (mean $IC_{50=}$ 20 μM). The good activity on tau aggregation, observed in sixteen out of twenty tested compounds bearing a methyl or a nitro group at position 4 of the tricyclic system, is even higher when an additional substituent (OH or OCH_3) is present in position 7. Among the 4-amino derivatives examined, only 7-unsubstituted compound (**16**) was active, in contrast with foregoing considerations. All the seven basic side chains, linked to the 1-amino group, were consistent with the inhibition of tau protein aggregation, but the highest potencies were observed for bulkier chains, like the [3-(quinolizidin-1-yl)propyl] and, particularly, [2-(1-methylpiperidin-4-yl)ethyl], suggesting a key role for the two nitrogen atoms separated by five carbon atoms. Comparing the thioxanthen-9-one and xanthen-9-one scaffolds, the sulfur bridge of the former seems to be more suitable for tau aggregation inhibition than the oxygen atom (**23**–**25**), as already observed [46] for the inhibition of Aβ aggregation.

2.3. Neuroprotective effect against okadaic acid-induced tau toxicity

The hyperphosphorylation of tau leading to neurofibrillary tangles (NFT) is one of the key pathological hallmarks of AD. The dephosphorylation of phospho-tau is mainly mediated by protein phosphatases (PPs), among which PP2A is considered the major phosphatase *in vivo* [62]. In some areas of AD brain, both the expression and activity of PP2A have been reported to be reduced whilst the kinase-mediated tau phosphorylation is increased. In this context, we hypothesized that the most promising tau inhibitor **20** could exert a neuroprotective effect against tau-induced toxicity. To test this hypothesis, human neuroblastoma SH-SY5Y cells were incubated for 24 h with a PP2A inhibitor, the okadaic acid (OA) [62], to induce tau phosphorylation, in the presence of **20** in the concentrations range 0.1–50 μM. Then, cell viability was evaluated by MTT assay, and the results were reported as % of cell viability referred to untreated cells (CTRL) as shown in Fig. 4. Estradiol and PD38, a known inhibitor of MAPK pathway, were used as positive controls. Notably, compound **20** demonstrated the ability to restore cell

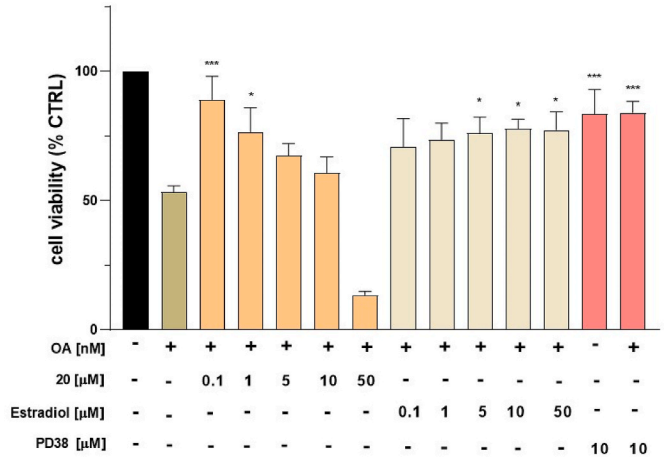

Fig. 4. Neuroblastoma cell line SH-SY5Y were incubated for 24 h with okadaic acid (100 nM) in the presence of the compounds tested. Then cell viability was evaluated by MTT assay, and the results were reported as % of cell viability referred to untreated cells (CTRL). Estradiol and PD38 were used as positive controls. Results represent the mean ± SD of three independent experiments. (One-way analysis of variance (ANOVA) followed by the Dunnett's test *p < 0.1, **p < 0.01, ***p < 0.001). (GraphPad Prism version 5).

viability counteracting tau-induced toxicity even at the low-test concentrations. In fact, from 0.1 to 10 μM compound **20** exhibited a potent neuroprotective effect comparable to that of estradiol and PD38, whereas at superior concentrations the cell viability decreased, probably because of its intrinsic toxicity (see section 2.6, Cytotoxicity profile).

2.4. Inhibition of human AChE and BChE

Bearing in mind the inhibition activity of thioxanthenone and xanthenone derivatives towards electric eel AChE and equine serum BChE (*ee*AChE and *es*BChE), we tested the most promising compounds also against human enzymes to confirm their inhibitory behavior (Table 2). The newly synthesized derivative **20** and compounds **6** and **9** (not previously tested) were also considered in the *in vitro* screening (Tables 1 and 2), resulting to be potent DBS inhibitors of ChEs (BChE preferring) and Aβ aggregation (IC_{50} = 1.3–2.45 μM), in accordance with the observations previously made [46]. Interestingly, the compounds demonstrated to be dual targeting agents also against human ChE isoforms with a preferential inhibition activity for *h*BChE. Whereas *h*AChE IC_{50} values fell in the low micromolar range, those *versus* *h*BChE mainly reached sub-micromolar potencies, or an outstanding nanomolar potency recorded for compound **4** (IC_{50} = 7 nM), which resulted the most potent *h*BChE inhibitor as well as highly selective over *h*AChE. Inhibition kinetics of **4** disclosed a mixed-type inhibitory mechanism, a typical feature of DBS inhibitors of ChEs (Fig. 5). The linker of five units between the thioxanthenone scaffold and the quinolizidine ring of compound **4** resulted as the best suited moiety, while the influence on inhibition potency exerted by substituents R^4 and R^7 appeared as less significant. Conversely, the replacement of the bulkier and high lipophilic quinolizidine ring with the *N*-methylpiperidine moiety in compound **20** was responsible for the breaking down of *h*BChE inhibition (16% inhibition at 10 μM), while preserving the ability to efficiently target the *es*BChE (IC_{50} = 0.96 μM). The analysis of interspecies activity profile revealed an inhibitory potency decrease passing from animal to human enzymes, although with a few exceptions as for **4** and **9**, which were about 10- and 1.5-folds more active against *h*BChE and *h*AChE, respectively. Hence, the present biological findings strengthen the overall merit of these chemotypes which were able to provide promising multitarget activity, including both AChE and BChE inhibition, acknowledged as early and advanced stage targets to treat AD.

2.5. Molecular modelling studies

To gain insight into the interaction of the compounds into the *h*BChE active site (PDB code: 1P0I), we performed a computational assessment of the best ligand of the series, the quinolizidinyl derivative **4**, compared to its piperidinyl analogue **20**. The comparison between the optimum binding pose obtained for each protonated compound suggested that compounds **4** and **20** share common stabilizing interactions but also some important dissimilarities in binding the esterase. To confirm and to corroborate the docking result and understand the different behaviors of the two compounds in the enzymatic assay (Table 2), we performed 100 ns of molecular dynamics (MD) simulation of the E-I complexes in explicit solvent. Finally, the corresponding ligand/protein free energy of binding (ΔG) and the specific enthalpic contribution for the main effective protein residues (ΔH_{res}) were calculated through MM/PBSA (Molecular Mechanics/Poisson Boltzmann Surface Area) analysis and PRBFED (per-residue binding free energy deconvolution) analysis, respectively. From the equilibrated MD trajectories (Fig. 6A and B), it arose that the similar thioxanthenone moieties showed the same interactions pattern for both **4** and **20** derivatives.

Specifically, the three condensate rings are perfectly lodged in the hydrophobic cavity lined by *h*BChE residues L314, F357, and F426 with a total enthalpy contribution of −2.78 kcal/mol and −3.03 kcal/mol (Fig. 6C) for **4** and **20**, respectively. Further favorable interactions are given by residues W110 and W259 through van der Waals and π-π stabilizations with the aromatic counterpart in the thioxanthenone ring. As shown in Fig. 6C, even these $\Sigma\Delta H_{res}$ are very comparable for both inhibitors, and they correspond to −3.58 kcal/mol for **4** and -3.62 kcal/mol for **20**. Eventually, the most relevant differences in *h*BChE binding between **4** and **20** rely on their protonated rings' binding performances. In fact, the quinolizine moiety of **4** are able to create two crucial specific interactions with *h*BChE: i) a stable π-cation interaction between its positively charged nitrogen atom and the aromatic side chain of Y360 (ΔH_{res} = −2.51 kcal/mol); and ii) a permanent hydrogen bond between the same basic nitrogen atom and the carboxylic group of D98, oriented in an optimal position by virtue of other two hydrogen bonds with S100 and S017 (Fig. 6A, $\Sigma\Delta H_{res}$ = −3.04 kcal/mol). On the other hand, the piperidine ring cannot exploit the same stabilizing scheme with the *h*BChE residues; given its shorter ethyl spacer, indeed, the piperidine nitrogen atom can provide only a stable hydrogen bond with the hydroxyl group of T148 (Fig. 6B, ΔH_{res} = −2.09 kcal/mol). Accordingly, the final calculated free energies of binding against *h*BChE were −9.83 kcal/mol and −7.49 kcal/mol for **4** and **20**, respectively (Fig. 6D), in agreement with their different inhibition potencies in the enzymatic assay (Table 2).

Table 2
Inhibitory activities of representative thioxanthenone and xanthenone derivatives against AChE and BChE from different species.

	IC_{50} (μM)[a]			
	*ee*AChE[b]	*h*AChE	*es*BChE[b]	*h*BChE
4	0.18	7.84 ± 0.86	0.088	0.0070 ± 0.0005
6	3.2 ± 0.1	4.26 ± 0.59	0.16 ± 0.01	0.90 ± 0.04
9	5.1 ± 1.2	3.59 ± 0.47	0.14 ± 0.03	0.71 ± 0.11
14	2.3	4.75 ± 0.54	0.15	1.82 ± 0.27
15	0.12	1.75 ± 0.30	2.0	7.31 ± 0.85
18	1.9	2.40 ± 0.73	0.15	0.99 ± 0.08
20	4.4 ± 0.1	16.10 ± 0.90	0.96 ± 0.15	(16 ± 1)[c]
25	0.14	8.81 ± 0.50	0.37	0.30 ± 0.04
Donepezil	0.020	0.017 ± 0.002	1.90	4.80 ± 1.00

[a] Values are means of three independent experiments.
[b] IC_{50} values for *ee*AChE and *es*BChE are from Ref. [46], except for the newly tested compounds **6**, **9** and **20**.
[c] % inhibition at 10 μM.

2.6. Cytotoxicity profile

Finally, cytotoxicity in primary mouse cortical cells was examined, at four concentrations (2.5, 5, 10 and 30 μM) for three compounds (Table 3), which were, respectively, the most (**20**), the least (**12**) and a middle potent (**10**) inhibitor of tau aggregation; compound **20** was also proven to be a potent inhibitor of Aβ aggregation.

Compounds **12** and **20** (the least and the most potent inhibitor of tau aggregation) reached the maximal toxicity (~80% death) after 24 h of incubation, which practically remained unchanged up to 72 h of exposure. On the other hand, compound **10** (a middle potent inhibitor) exhibited the lowest toxicity, causing, only after 72 h of incubation, the 34–54% of mortality in relation to the concentration tested. A similar trend may be observed by correlating the $A\beta_{40}$ inhibition to cytotoxicity. These results suggest that only a weak correlation may exist, if any, between cytotoxicity and inhibition potency for aggregation of both proteins.

Concentrations used in this toxicity test were close to some of the IC_{50} values for the inhibition of tau and Aβ aggregation, indicating a rather narrow safety margin. Moderate safety windows were also observed, taking into account the cytotoxicity previously determined for compound **2** *versus* the human neuroblastoma cell line SH-SY5Y (IC_{50} = 7.22 μM) [46], and for compounds **1**, **2** and **19** *versus* the monkey kidney Vero76 cells (IC_{50} within the range 12.4–23.5 μM) [55]. It is worth noting that compound **19** (lucanthone), while displaying an IC_{50} = 12.4 μM against Vero76 cells, was safely used in the past for the therapy of

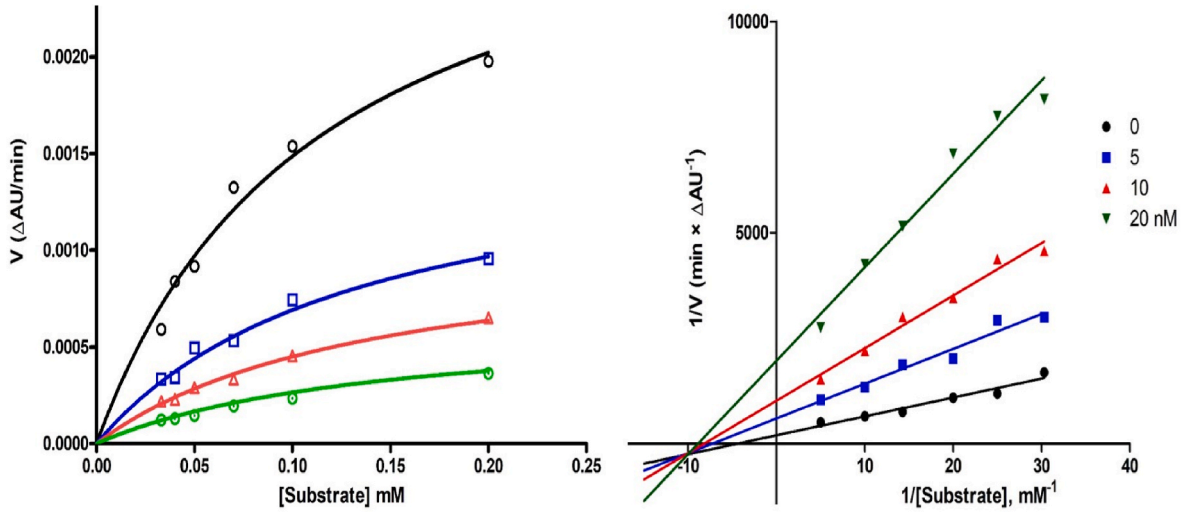

Fig. 5. Michaelis-Menten (left) and Lineweaver-Burk (right) plots of *h*BChE inhibition exerted by **4**.

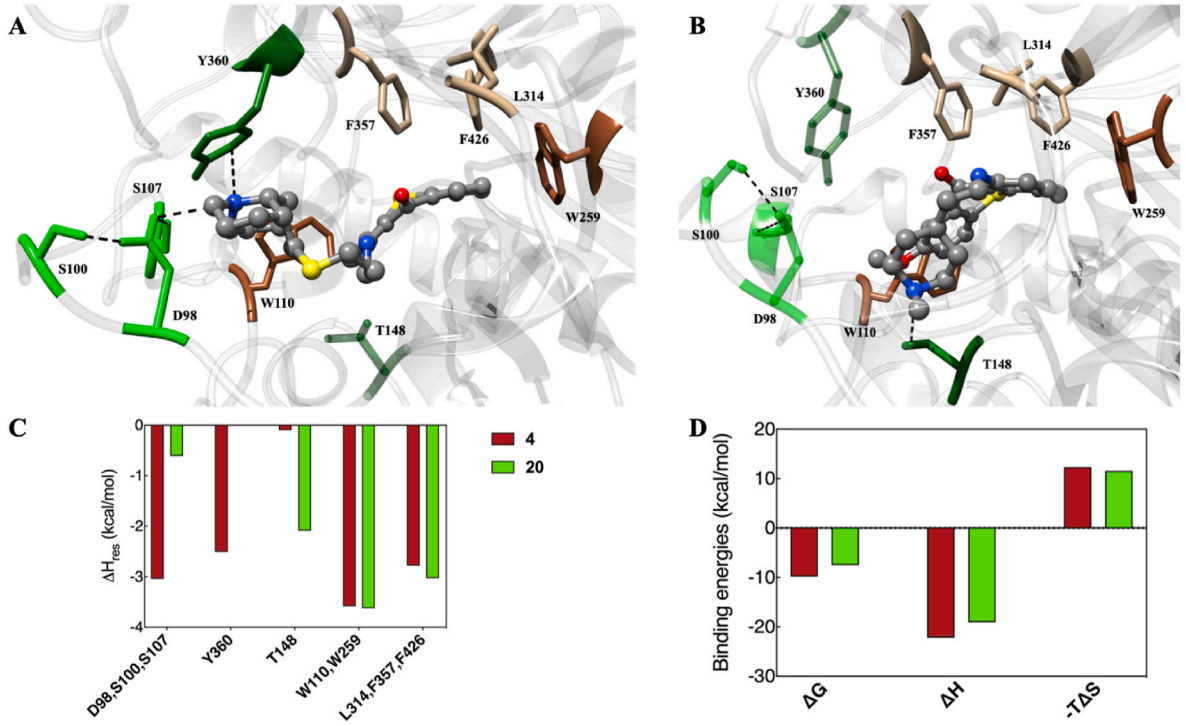

Fig. 6. Details of binding interactions of compounds **4** (A) and **20** (B) in the binding pocket of *h*BChE. Both ligands are shown as atom-colored sticks-and-balls (C, grey, N, blue, O, red) while the side chains of protein residues mainly interacting with the two compounds are depicted as colored sticks and labeled. Hydrogen atoms, water molecules, and ions are omitted for clarity. (B) Comparison between *h*BChE per-residue analysis of compound **4** (firebrick) against **20** (green). (C) Comparison between the calculated free energy of binding (ΔG) and its components of compound **4** (firebrick) against **20** (green).

schistosomiasis up to 2–3 g per daily dose [63].

Undergoing studies have already revealed that compound **2** displays low toxicity against primary cultures of cerebellar granule cells from postnatal rats (P7) [78% viability at 10 μM, in comparison with vehicle-treated control], whilst compound **20**, the most active against tau aggregation seems to be toxic against this cell line [30% cell viability at 10 μM].

By comparing the present data collected in Tables 1 and 2 with previous ones, it may be observed that the eight best dual inhibitors of tau (IC_{50} within the range: 1.8–9.1 μM, mean IC_{50} = 6.0 μM) and Aβ aggregation (IC_{50} in the range: 1.3–9.1 μM, mean IC_{50} = 4.5 μM) also exhibited low micromolar or submicromolar inhibition of *h*AChE (IC_{50} range: 0.12–7.6 μM, mean IC_{50} = 4.19 μM) and BChE (IC_{50} range: 0.15–2.0 μM, mean IC_{50} = 0.91 μM), thus representing interesting multitarget leads for AD therapy. Therefore, the biological multifunctional profile experienced by these compounds well matches with that of lead compounds at the early stages of anti-AD drug development. Anyhow, for a more meaningful assessment of the therapeutic potential of the present compounds, the issue of their *in vitro* and *in vivo* toxicity, in comparison with licensed drugs for AD should be further investigated.

3. Conclusions

A set of twenty-five thioxanthene-9-one and xanthen-9-one

Table 3
Cytotoxicity of compounds **10**, **12** and **20** at different concentrations in primary mouse cortical cultures. Results represent the mean of three independent experiments; SEM < 10%.

Compd.	Conc.	% cellular death after *n* hours of incubation								
	(μM)	1	2	3	4	5	6	24	48	72
10	2.5	−0.1	1.6	1.8	2.2	1.9	2.0	8.9	18.4	33.6
	5	1.0	3.4	1.8	3.3	4.4	5.7	17.8	27.8	37.6
	10	4.2	5.8	4.9	5.3	6.1	4.0	19.6	27.4	42.1
	30	3.8	5.7	7.1	9.5	9.3	10.7	48.6	52.4	54.3
12	2.5	0.3	3.1	3.7	4.7	5.2	5.2	85.5	83.3	79.6
	5	1.6	2.9	5.0	4.3	6.6	5.7	77.0	72.4	79.4
	10	−3.1	1.7	6.4	16.2	31.0	35.9	86.1	79.1	74.8
	30	11.6	19.1	29.7	42.0	51.0	54.3	82.1	82.9	80.8
20	2.5	2.9	3.8	8.5	17.4	23.8	29.9	76.2	81.5	77.8
	5	1.6	7.6	15.8	25.8	32.6	41.4	91.3	85.6	85.7
	10	16.7	43.5	48.9	52.6	54.4	55.7	88.5	84.1	92.4
	30	28.5	46.5	54.7	56.1	60.4	61.9	86.1	88.1	89.4

derivatives, that were previously shown to inhibit ChEs and $A\beta_{40}$ aggregation [46], were evaluated for the inhibition of tau protein aggregation. All compounds exhibited a good activity, ten of them displaying IC_{50} values lower than 10 μM. Eight of these compounds (**5**–**8**, **10**, **14**, **15** and **20**) shared comparable micromolar inhibitory potency *versus* Aβ aggregation and *h*AChE, while inhibiting *h*BChE even at submicromolar concentration. The newly designed and synthesized compound **20** showed outstanding biological data, inhibiting tau protein and Aβ aggregation with IC_{50} = 1.8 and 1.3 μM, respectively, and *ee*AChE and *h*BChE with IC_{50} = 4.4 and 0.96 μM, respectively. Also compounds **10** and **15** are noteworthy, particularly the former one, which associated a valuable activity with only a modest cytotoxicity.

It is to underline also the exceptionally high selectivity of compound **4** for *h*BChE *versus* *h*AChE (three order of magnitude). This result was very interesting, considering the growing importance in the AD potential therapy of the BChE inhibition, which, besides its symptomatic efficacy, seems to display some DMT effects [64,65]. The long linker chain (that characterizes compound **4**) represents a structural feature to be further challenged for improving BChE inhibition.

The observed balance of the inhibitory potencies *versus* the relevant targets fulfills a fundamental requisite for multitarget compounds to tackle the network of pathogenic pathways of AD more efficiently. Preliminary *in vitro* assays for cytotoxicity of some compounds indicated a narrow safety margin, which deserves a more in-depth investigation with a goal to establishing the value of the present, otherwise very promising, compounds as potential MTDLs for AD therapy. Indeed, further structural variations are currently under investigation in our lab aiming at the identification of those chemical features which are able to maintain a good multitarget activity profile while decreasing potential cytotoxic effects of our compounds.

4. Experimental section

4.1. Chemistry

4.1.1. General methods

Chemicals and solvents were purchased from Sigma-Aldrich or Zentek (Milan, Italy). Melting points were determined using a Büchi apparatus and are uncorrected. ^{1}H NMR spectra and ^{13}C NMR spectra were recorded using a Jeol instrument at 400 and 101 MHz, respectively; chemical shifts are reported as δ (ppm) and are referenced to $CDCl_3$ signal: singlet at 7.26 ppm (^{1}H), triplet at 77.0 ppm (^{13}C); J are expressed in Hz. Elemental analyses were performed on a Flash 2000 CHNS (Thermo Scientific) instrument in the Microanalysis Laboratory of the Department of Pharmacy, University of Genoa.

4.1.2. Synthesis of 7-methoxy-4-methyl-1-[2-(1-methylpiperidin-4-yl)ethylamino]-9H-thioxanthen-9-one (20)

A mixture of 1-chloro-7-methoxy-4-methyl-9*H*-thioxanthen-9-one [57] (0.38 g, 1.3 mmol) with 2-(1-methylpiperidin-4-yl)ethan-1-amine (g 0.37, 2.6 mmol) was heated at 170 °C in a sealed tube for 6 h. Then the reaction mixture was treated with 2 N HCl and extracted with Et_2O in order to remove the unreacted thioxanthenone. The acid solution was then alkalinized with 6 N NaOH, and thoroughly extracted with CH_2Cl_2. After drying (anh. Na_2SO_4), the organic layer was evaporated to dryness affording a residue that was purified by CC (SiO_2/CH_2Cl_2+2%DEA).

Yield: 50%. Mp. 110.7–112.4 °C. ^{1}H NMR (400 MHz, $CDCl_3$): δ 10.17 (s, 1H, NH), 7.96 (d, J = 2.9 Hz, 1H, H(8) thioxanthenone), 7.43 (d, J = 8.7 Hz, 1H, H(5) thioxanthenone), 7.25 (d superimposed to solvent peak, J = 9.4 Hz, 1H, H(3) thioxanthenone), 7.20 (dd, J = 8.7, 2.9 Hz, 1H, H(6) thioxanthenone), 6.50 (d, J = 8.5 Hz, 1H, H(2) thioxanthenone), 3.92 (s, 3H, OC$\underline{H_3}$), 3.53 (d, J = 11.7 Hz, 2H, NHC$\underline{H_2}$CH$_2$), 3.34–3.22 (m, 2H(α) of C2/C6-piperidine), 2.83–2.66 (m, 5H, 2H(β) of C2/C6-piperidine superimposed to 2.76, 3H, d, J = 4.4 Hz, CH_3-Arom.), 2.32 (s, 3H, N–C$\underline{H_3}$), 2.07–1.91 (m, 4H, C3/C5-piperidine), 1.85–1.75 (m, 3H, 2H NHCH$_2$C$\underline{H_2}$ and 1H of C4-piperidine). ^{13}C NMR (101 MHz, $CDCl_3$): δ 183.27, 158.41, 152.32, 138.41, 135.58, 131.27, 128.29, 127.00, 121.97, 118.50, 112.60, 110.03, 106.50, 55.76, 54.99 (2C), 44.03, 39.79, 34.19, 31.27, 29.12 (2C), 19.24. Anal. Calcd for $C_{23}H_{28}N_2O_2S$: C 69.66; H 7.12; N 7.06; S 8.08. Found: C 69.51; H 6.96; N 6.76; S 7.78.

4.2. Biological assays

4.2.1. General methods

All reagents were purchased from Sigma Aldrich (Milan, Italy), unless otherwise specified. Assays were performed in Greiner 96-well plates (Greiner Bio-One GmbH, Frickenhausen, Germany) and read with Infinite M1000 Pro (Tecan, Cernusco sul Naviglio, Italy). Experiments were run in triplicate. Results were expressed by statistical analysis while IC_{50}s were obtained by nonlinear regression using Prism software (GraphPad Prism version 5.00 for Windows, GraphPad Software, San Diego, CA, USA).

4.2.2. Inhibition of PHF6 aggregation

The assay was based on the decrease of ThT fluorescence after binding of 10 μM inhibitor to 50 μM PHF6 sequence (JPT Peptide Technologies GmbH, Berlin, Germany). The experimental procedure has been already described [51,58].

4.2.3. Inhibition of $A\beta_{40}$ aggregation

A fluorescence-based method for enhanced amyloid aggregation of $A\beta_{40}$ peptide (EzBiolab, Carmel, IN, USA), using 2% HFIP as aggregation enhancer and thioflavin T (ThT) as the fluorescent dye, was used as

already described [66].

4.2.4. Inhibition of cholinesterases

In vitro inhibition assays were performed with the Ellman's spectrophotometric method, by applying already published procedures [46,47,51]. For inhibition kinetics, four concentrations of **4** (0–20 nM) and six of substrate acetylthiocoline (ranging from 33 to 200 μM) were used. Inhibition constants were calculated by nonlinear regression using the above mentioned Prism software.

4.2.5. In vitro cell-based assays

Compounds for bacterial media were purchased from CondaLab (Madrid, Spain). M9 minimal medium; for 100 mL: 10 mL salts 10 × (0.68 g Na_2HPO_4, 0.30 g KH_2PO_4, 0.05 g NaCl, 0.10 g NH_4Cl), 0.2 mL (1 M $MgSO_4$), 0.2 mL (50 mM $CaCl_2$), 2.5 mL (20% glucose) and 87.1 mL (H_2O).

4.2.6. Tau aggregation inhibition assay in bacterial cells

Escherichia coli competent cells BL21 (DE3) were transformed with pTARA containing the RNA-polymerase gen of T7 phage (T7RP) under the control of the promoter PBAD and pRKT42 vector encoding four repeats of tau protein in two inserts. Because of the addition of the initiation codon ATG in front of gene, the over-expressed protein contains an additional methionine residue at its N terminus. Tau anti-aggregating activities of the target compounds were assessed in *E. coli* cells, as previously described [52,60]. M9 minimal medium (10 mL) containing 0.5% of glucose, 100 μg/mL of ampicillin and 12.5 μg/mL of chloramphenicol was inoculated with a colony of BL21 (DE3) cells bearing the plasmids. To fresh M9 minimal medium containing 0.5% of glucose, 50 μg/mL of ampicillin, 12.5 μg/mL of chloramphenicol, and 250 μM of ThS, the volume of overnight culture necessary to get a 1:500 dilution was added. The cultures were grown at 37 °C and 250 rpm overnight until cell density reached $OD_{600} = 0.6$. A volume of 980 μL of the cultures was transferred into 1.5 mL Eppendorf tubes that contained 10 μL of a solution of the target compound in DMSO and 10 μL of arabinose at 25%, leading to a final inhibitor concentration of 10 μM. The resulting cultures were grown at 37 °C and 1400 rpm with a Thermomixer (Eppendorf, Hamburg, Germany) overnight. The same amount of DMSO without the target compound was added to the sample as a negative control (maximal amount of tau), whereas non-induced samples (in the absence of arabinose) were prepared as positive controls (absence of tau), and to assess the potential intrinsic toxicity of the target compounds. In addition, the absorbance at 600 nm of these samples was assessed to confirm the correct bacterial growth, discarding potential intrinsic toxicity of compounds. To determine the IC_{50} values, the same protocol was followed but only modifying the initial concentration of compounds. In order to use different final concentrations of compound, we performed a dilutions banc from a stock solution of 100 mM in MilliQ H_2O.

4.2.7. Thioflavin S steady-state fluorescence

ThS fluorescence and absorbance were tracked using a DTX 800 plate reader Multimode Detector equipped with a Multimode Analysis Software (Beckman-Coulter, Indianapolis, IN, USA). Filters of 430/35 and 485/20 nm were used for the excitation and emission wavelengths, respectively. 620/8 nm filters were also used for the absorbance determination. It should be stressed that ThS fluorescence normalization was carried out considering as 100% the ThS fluorescence of the bacterial cells expressing tau in the absence of compounds and 0% the ThS fluorescence of the bacterial cells non-expressing tau.

4.2.8. Primary embryonic cortical cultures

Primary cortical cultures were prepared from 16.5 mouse embryo (E16.5) brains. Briefly, cortical regions were dissected and washed in ice-cold 0.1 M phosphate buffered saline (PBS) containing 6.5 mg/mL glucose. Tissue pieces were trypsinized for 15 min at 37 °C. After addition of 1/3 inactivated horse serum (v/total volume) followed by centrifugation, cells were dissociated by trituration in 0.1 M PBS containing 0.025% DNase with a pipette (all from Sigma- Aldrich). Dissociated cells were plated at ≈ 3000 cells/mm^2 on 24-well Nunc plates (Denmark) coated with poly-D-lysine (Sigma-Aldrich). The culture medium was Neurobasal™ supplemented with 2 mM glutamine, 6.5 mg/mL glucose, antibiotics (Pen./Strept.), 5% inactivated horse serum, and B27 (Invitrogen-Thermo Fisher Scientific). Compounds were added to the cultures after 4 days *in vitro* (*DIV*).

4.2.9. Determination of cytotoxicity

Cell death was assessed using a slightly modified propidium iodide (PI) uptake method, as described by Enguita et al. [67]. Propidium iodide fluorescence was measured in 24-well plates using an Infinite M200 PRO scanner (TECAN). Spectrofluorometer analysis and settings were as follows: 530 nm excitation, 645 nm emission, and data recorded in relative fluorescence units. Baseline fluorescence F1 was measured 1 h after addition of propidium iodide (30 μM) as an index of cell death not related to the treatment. Subsequently, fluorescence readings were taken at different times after the onset of the treatment. At the end of the experiment, the cells were permeabilized for 10 min with 500 mM digitonin at 37 °C to obtain the maximum fluorescence corresponding to 100% of cell death (Fmax). The percentage of cell death was calculated as follows: % cell death = 100 × (Fn−F1)/(Fmax−F1), where Fn is the fluorescence at any given time [68].

4.2.10. Determination of neuroprotection from okadaic acid-induced tau toxicity

Human neuroblastoma SH-SY5Y cells were maintained in T-75 flasks in Dulbecco's modified Eagle's medium (DMEM) supplemented with 100 U/mL penicillin, 100 μg/mL streptomycin, 10% FBS, at 37.0 °C, 5% CO_2. At 80% of confluence, cells were removed by mechanical stirring and plated at $4{,}5 \times 10^4$ cells per well in a 96-well plate. To examine the potential protective effect of **20** against the cytotoxic effect of okadaic-acid (OA), a potent and specific inhibitor of serine/threonine phosphatase (PP), 80% confluent SH-SY5Y cells were plated in a 96 well/plate and incubated with compound at concentrations ranging from 0.1 to 50 μM in the presence of OA 100 nM for 24h, at 37 °C, 5% CO_2. After incubation, the medium was removed and the cytoprotective effect was assessed by evaluating cell viability through the MTT assay. Controls were represented by cells treated with OA alone, by standard estradiol used at the same concentrations of **20**, PD38 (an inhibitor of MAPK pathway) and by untreated cells (CTRL). The results were expressed as percentage of cell survival compared to untreated cells (CTRL).

Data analysis was performed by using GraphPad Prism 5.0. The data are expressed as mean values ± SD. Statistical analysis was carried out using one-way analysis of variance (ANOVA) followed by the Dunnett's Multiple Comparison post hoc test for multiple comparison analysis. Levels of significance are reported towards the cytotoxic insult represented by OA.

4.3. Computational experimental details

All simulations were carried our using Amber 21 [69] running on our own CPU/GPU cluster. All images were created by the UCSF Chimera software [70], and graphs were produced by GraphPad Prism 8 (GraphPad Software, San Diego, California USA, www.graphpad.com). The starting molecular structure of hBChE was obtained from the Protein Data Bank (PDB code: 1P0I) [71]. Docking and classical Molecular Dynamics simulations on *h*BChE in complex with compounds **4** and **20** were carried out following a well validated procedure [51,72,73]. Briefly, the geometry- and energy-optimized structures of compounds **4** and **20** were docked into each identified hBChE binding pocket using Autodock 4.2.6/Autodock Tools 1.4.6161 [74] on a win 64 platform. The resulting complexes were solvated with explicit TIP3P [75] water and then, the system density and volume were relaxed in NPT ensemble

maintaining the Berendsen barostat for 20 ns. After this step, 100 ns of unrestrained NVT production simulation was run for each system. Following the MM/PBSA approach [76] each binding free energy values (ΔG) were calculated as the sum of the enthalpic (ΔH) and entropic contributions (TΔS). The per-residue binding free energy decomposition (ΔH_{res}) analysis was carried out using the Molecular Mechanics/Generalized Boltzmann Surface Area (MM/GBSA) approach [77] and was based on the same snapshots used in the binding free energy calculation.

Declaration of competing interest

The authors declare that they have no known competing financial interests or personal relationships that could have appeared to influence the work reported in this paper.

Data availability

The authors are unable or have chosen not to specify which data has been used.

Acknowledgements

J.A. del Río and R. Gavín were supported by PRPCDEVTAU (PID2021-123714OB-I00), ALTERNED (PLEC2022-009401) and PDC2022-133268-I00 funded by MCIN/AEI/10.13039/501100011033 and by "ERDF A way of making Europe", the CERCA Programme, and by AGAUR (SGR2021-00453). The project leading to these results received funding from "la Caixa" Foundation (ID 100010434) under the agreement LCF/PR/HR19/52160007 to JADR.

Appendix A. Supplementary data

Supplementary data to this article can be found online at https://doi.org/10.1016/j.ejmech.2023.115169.

References

[1] Z. Breijyeh, R. Karaman, Comprehensive review on alzheimer's disease: causes and treatment, Molecules 25 (2020) 5789, https://doi.org/10.3390/molecules25245789.
[2] L. Blaikie, G. Kay, P. Kong Thoo Lin, Current and emerging therapeutic targets of alzheimer's disease for the design of multi-target directed ligands, Med. chem. commun 10 (2019) 2052–2072, https://doi.org/10.1039/c9md00337a.
[3] Z. Fišar, Linking the amyloid, tau, and mitochondrial hypotheses of alzheimer's disease and identifying promising drug targets, Biomolecules 12 (2022) 1676, https://doi.org/10.3390/biom12111676.
[4] I.W. Hamley, The amyloid beta peptide: a chemist's perspective. Role in Alzheimer's and fibrillization, Chem. Rev. 112 (2012) 5147–5192, https://doi.org/10.1021/cr3000994.
[5] G. Marucci, M. Buccioni, D.D. Ben, C. Lambertucci, R. Volpini, F. Amenta, Efficacy of acetylcholinesterase inhibitors in Alzheimer's disease, Neuropharmacology 190 (2021), 108352, https://doi.org/10.1016/j.neuropharm.2020.108352.
[6] M. Catto, A.A. Berezin, D. Lo Re, G. Loizou, M. Demetriades, A. De Stradis, F. Campagna, P.A. Koutentis, A. Carotti, Design, synthesis and biological evaluation of benzo[e][1,2,4]triazin-7(1H)-one and [1,2,4]-triazino[5,6,1-jk] carbazol-6-one derivatives as dual inhibitors of beta-amyloid aggregation and acetyl/butyryl cholinesterase, Eur. J. Med. Chem. 58 (2012) 84–97, https://doi.org/10.1016/j.ejmech.2012.10.003.
[7] J.L. Domínguez, F. Fernández-Nieto, M. Castro, M. Catto, M.R. Paleo, S. Porto, F. J. Sardina, J.M. Brea, A. Carotti, M.C. Villaverde, F. Sussman, Computer-aided structure-based design of multitarget leads for Alzheimer's disease, J. Chem. Inf. Model. 55 (2015) 135–148, https://doi.org/10.1021/ci500555g.
[8] S. Agatonovic-Kustrin, C. Kettle, D.W. Morton, A molecular approach in drug development for Alzheimer's disease, Biomed. Pharmacother. 106 (2018) 553–565, https://doi.org/10.1016/j.biopha.2018.06.147.
[9] P. Yang, F. Sun, Aducanumab: the first targeted Alzheimer's therapy, Drug. Discov. Ther. 15 (2021) 166–168, https://doi.org/10.5582/ddt.2021.01061.
[10] M. Prillaman, Alzheimer's drug slows mental decline in trial - but is it a breakthrough? Nature 610 (2022) 15–16, https://doi.org/10.1038/d41586-022-03081-0.
[11] D. Jeremic, L. Jiménez-Díaz, J.D. Navarro-López, Past, present and future of therapeutic strategies against amyloid-β peptides in Alzheimer's disease: a systematic review, Ageing Res. Rev. 72 (2021), 101496, https://doi.org/10.1016/j.arr.2021.101496.
[12] M.A. Busche, B.T. Hyman, Synergy between amyloid-β and tau in Alzheimer's disease, Nat. Neurosci. 23 (2020) 1183–1193, https://doi.org/10.1038/s41593-020-0687-6.
[13] D. Malafaia, H.M.T. Albuquerque, A.M.S. Silva, Amyloid-β and tau aggregation dual-inhibitors: a synthetic and structure-activity relationship focused review, Eur. J. Med. Chem. 214 (2021), 113209, https://doi.org/10.1016/j.ejmech.2021.113209.
[14] Á. Sebastián-Serrano, L. de Diego-García, M. Díaz-Hernández, The neurotoxic role of extracellular tau protein, Int. J. Mol. Sci. 19 (2018) E998, https://doi.org/10.3390/ijms19040998.
[15] J.L. Hoskin, M.N. Sabbagh, Y. Al-Hasan, B. Decourt, Tau immunotherapies for Alzheimer's disease, Expet Opin. Invest. Drugs 28 (2019) 545–554, https://doi.org/10.1080/13543784.2019.1619694.
[16] C.M. Wischik, C.R. Harrington, J.M.D. Storey, Tau-aggregation inhibitor therapy for Alzheimer's disease, Biochem. Pharmacol. 88 (2014) 529–539, https://doi.org/10.1016/j.bcp.2013.12.008.
[17] N. Guzior, A. Wieckowska, D. Panek, B. Malawska, Recent development of multifunctional agents as potential drug candidates for the treatment of Alzheimer's disease, Curr. Med. Chem. 22 (2015) 373–404, https://doi.org/10.2174/0929867321666141106122628.
[18] P. Michalska, I. Buendia, L. Del Barrio, R. Leon, Novel multitarget hybrid compounds for the treatment of alzheimer's disease, Curr. Top. Med. Chem. 17 (2017) 1027–1043, https://doi.org/10.2174/1568026616666160927154116.
[19] M.G. Savelieff, G. Nam, J. Kang, H.J. Lee, M. Lee, M.H. Lim, Development of multifunctional molecules as potential therapeutic candidates for alzheimer's disease, Parkinson's disease, and amyotrophic lateral sclerosis in the last decade, Chem. Rev. 119 (2019) 1221–1322, https://doi.org/10.1021/acs.chemrev.8b00138.
[20] S. Jadhav, J. Avila, M. Schöll, G.G. Kovacs, E. Kövari, R. Skrabana, L.D. Evans, E. Kontsekova, B. Malawska, R. de Silva, L. Buee, N. Zilka, A walk through tau therapeutic strategies, Acta. Neuropathol. Commun. 7 (2019) 22, https://doi.org/10.1186/s40478-019-0664-z.
[21] C.L. Sayas, Chapter 10 - tau-based therapies for Alzheimer's disease: promising novel neuroprotective approaches, in: I. Gozes, J. Levine (Eds.), Neuroprotection in Autism, Schizophrenia and Alzheimer's Disease, Academic Press, 2020, pp. 245–272, https://doi.org/10.1016/B978-0-12-814037-6.00005-7.
[22] G. Pandey, V. Ramakrishnan, Invasive and non-invasive therapies for Alzheimer's disease and other amyloidosis, Biophys.Rev. 12 (2020) 1175–1186, https://doi.org/10.1007/s12551-020-00752-y.
[23] L. Wang, null Bharti, R. Kumar, P.F. Pavlov, B. Winblad, Small molecule therapeutics for tauopathy in Alzheimer's disease: walking on the path of most resistance, Eur. J. Med. Chem. 209 (2021), 112915, https://doi.org/10.1016/j.ejmech.2020.112915.
[24] H. Ashrafian, E.H. Zadeh, R.H. Khan, Review on Alzheimer's disease: inhibition of amyloid beta and tau tangle formation, Int. J. Biol. Macromol. 167 (2021) 382–394, https://doi.org/10.1016/j.ijbiomac.2020.11.192.
[25] A. Beato, A. Gori, B. Boucherle, M. Peuchmaur, R. Haudecoeur, β-Carboline as a privileged scaffold for multitarget strategies in alzheimer's disease therapy, J. Med. Chem. 64 (2021) 1392–1422, https://doi.org/10.1021/acs.jmedchem.0c01887.
[26] M. Okuda, I. Hijikuro, Y. Fujita, T. Teruya, H. Kawakami, T. Takahashi, H. Sugimoto, Design and synthesis of curcumin derivatives as tau and amyloid β dual aggregation inhibitors, Bioorg. Med. Chem. Lett 26 (2016) 5024–5028, https://doi.org/10.1016/j.bmcl.2016.08.092.
[27] M. Convertino, R. Pellarin, M. Catto, A. Carotti, A. Caflisch, 9,10-Anthraquinone hinders beta-aggregation: how does a small molecule interfere with Abeta-peptide amyloid fibrillation? Protein Sci. 18 (2009) 792–800, https://doi.org/10.1002/pro.87.
[28] K. Cisek, G.L. Cooper, C.J. Huseby, J. Kuret, Structure and mechanism of action of tau aggregation inhibitors, Curr. Alzheimer Res. 11 (2014) 918–927, https://doi.org/10.2174/1567205011666141107150331.
[29] K. Cisek, J.R. Jensen, N.S. Honson, K.N. Schafer, G.L. Cooper, J. Kuret, Ligand electronic properties modulate tau filament binding site density, Biophys. Chem. 170 (2012) 25–33, https://doi.org/10.1016/j.bpc.2012.09.001.
[30] S. Amslinger, The tunable functionality of alpha,beta-unsaturated carbonyl compounds enables their differential application in biological systems, ChemMedChem 5 (2010) 351–356, https://doi.org/10.1002/cmdc.200900499.
[31] M. Necula, C.N. Chirita, J. Kuret, Cyanine dye N744 inhibits tau fibrillization by blocking filament extension: implications for the treatment of tauopathic neurodegenerative diseases, Biochemistry 44 (2005) 10227–10237, https://doi.org/10.1021/bi050387o.
[32] B. Bulic, M. Pickhardt, E.-M. Mandelkow, E. Mandelkow, Tau protein and tau aggregation inhibitors, Neuropharmacology 59 (2010) 276–289, https://doi.org/10.1016/j.neuropharm.2010.01.016.
[33] M. Oz, D.E. Lorke, G.A. Petroianu, Methylene blue and Alzheimer's disease, Biochem. Pharmacol. 78 (2009) 927–932, https://doi.org/10.1016/j.bcp.2009.04.034.
[34] G.K. Wilcock, S. Gauthier, G.B. Frisoni, J. Jia, J.H. Hardlund, H.J. Moebius, P. Bentham, K.A. Kook, B.O. Schelter, D.J. Wischik, C.S. Davis, R.T. Staff, V. Vuksanovic, T. Ahearn, L. Bracoud, K. Shamsi, K. Marek, J. Seibyl, G. Riedel, J. M.D. Storey, C.R. Harrington, C.M. Wischik, Potential of low dose leuco-methylthioninium bis(hydromethanesulphonate) (LMTM) monotherapy for treatment of mild alzheimer's disease: cohort analysis as modified primary outcome in a phase III clinical trial, J Alzheim. Dis. 61 (2018) 435–457, https://doi.org/10.3233/JAD-170560.
[35] Y.-P. Chen, Z.-Y. Zhang, Y.-P. Li, D. Li, S.-L. Huang, L.-Q. Gu, J. Xu, Z.-S. Huang, Syntheses and evaluation of novel isoliquiritigenin derivatives as potential dual

inhibitors for amyloid-beta aggregation and 5-lipoxygenase, Eur. J. Med. Chem. 66 (2013) 22–31, https://doi.org/10.1016/j.ejmech.2013.05.015.
[36] K. Ono, Y. Yoshiike, A. Takashima, K. Hasegawa, H. Naiki, M. Yamada, Potent anti-amyloidogenic and fibril-destabilizing effects of polyphenols in vitro: implications for the prevention and therapeutics of Alzheimer's disease, J. Neurochem. 87 (2003) 172–181, https://doi.org/10.1046/j.1471-4159.2003.01976.x.
[37] W.M. Berhanu, A.E. Masunov, Natural polyphenols as inhibitors of amyloid aggregation. Molecular dynamics study of GNNQQNY heptapeptide decamer, Biophys. Chem. 149 (2010) 12–21, https://doi.org/10.1016/j.bpc.2010.03.003.
[38] A.R.A. Ladiwala, J.S. Dordick, P.M. Tessier, Aromatic small molecules remodel toxic soluble oligomers of amyloid beta through three independent pathways, J. Biol. Chem. 286 (2011) 3209–3218, https://doi.org/10.1074/jbc.M110.173856.
[39] R. Scherzer-Attali, R. Pellarin, M. Convertino, A. Frydman-Marom, N. Egoz-Matia, S. Peled, M. Levy-Sakin, D.E. Shalev, A. Caflisch, E. Gazit, D. Segal, Complete phenotypic recovery of an Alzheimer's disease model by a quinone-tryptophan hybrid aggregation inhibitor, PLoS One 5 (2010), e11101, https://doi.org/10.1371/journal.pone.0011101.
[40] G.K. Viswanathan, A. Paul, E. Gazit, D. Segal, Naphthoquinone tryptophan hybrids: a promising small molecule scaffold for mitigating aggregation of amyloidogenic proteins and peptides, Front. Cell Dev. Biol. 7 (2019) 242, https://doi.org/10.3389/fcell.2019.00242.
[41] M. Campora, V. Francesconi, S. Schenone, B. Tasso, M. Tonelli, Journey on naphthoquinone and anthraquinone derivatives: new insights in alzheimer's disease, Pharmaceuticals 14 (2021) 33, https://doi.org/10.3390/ph14010033.
[42] R. Colombo, A. Carotti, M. Catto, M. Racchi, C. Lanni, L. Verga, G. Caccialanza, E. De Lorenzi, CE can identify small molecules that selectively target soluble oligomers of amyloid beta protein and display antifibrillogenic activity, Electrophoresis 30 (2009) 1418–1429, https://doi.org/10.1002/elps.200800377.
[43] A. Gandini, M. Bartolini, D. Tedesco, L. Martinez-Gonzalez, C. Roca, N.E. Campillo, J. Zaldivar-Diez, C. Perez, G. Zuccheri, A. Miti, A. Feoli, S. Castellano, S. Petralla, B. Monti, M. Rossi, F. Moda, G. Legname, A. Martinez, M.L. Bolognesi, Tau-centric multitarget approach for alzheimer's disease: development of first-in-class dual glycogen synthase kinase 3β and tau-aggregation inhibitors, J. Med. Chem. 61 (2018) 7640–7656, https://doi.org/10.1021/acs.jmedchem.8b00610.
[44] R. Purgatorio, M. de Candia, A. De Palma, F. De Santis, L. Pisani, F. Campagna, S. Cellamare, C.D. Altomare, M. Catto, Insights into structure-activity relationships of 3-arylhydrazonoindolin-2-one derivatives for their multitarget activity on β-amyloid aggregation and neurotoxicity, Molecules 23 (2018) E1544, https://doi.org/10.3390/molecules23071544.
[45] S. Fuse, K. Matsumura, Y. Fujita, H. Sugimoto, T. Takahashi, Development of dual targeting inhibitors against aggregations of amyloid-β and tau protein, Eur. J. Med. Chem. 85 (2014) 228–234, https://doi.org/10.1016/j.ejmech.2014.07.095.
[46] M. Tonelli, M. Catto, B. Tasso, F. Novelli, C. Canu, G. Iusco, L. Pisani, A.D. Stradis, N. Denora, A. Sparatore, V. Boido, A. Carotti, F. Sparatore, Multitarget therapeutic leads for alzheimer's disease: quinolizidinyl derivatives of Bi- and tricyclic systems as dual inhibitors of cholinesterases and β-amyloid (Aβ) aggregation, ChemMedChem 10 (2015) 1040–1053, https://doi.org/10.1002/cmdc.201500104.
[47] B. Tasso, M. Catto, O. Nicolotti, F. Novelli, M. Tonelli, I. Giangreco, L. Pisani, A. Sparatore, V. Boido, A. Carotti, F. Sparatore, Quinolizidinyl derivatives of bi- and tricyclic systems as potent inhibitors of acetyl- and butyrylcholinesterase with potential in Alzheimer's disease, Eur. J. Med. Chem. 46 (2011) 2170–2184, https://doi.org/10.1016/j.ejmech.2011.02.071.
[48] Q. Li, Y. Chen, S. Xing, Q. Liao, B. Xiong, Y. Wang, W. Lu, S. He, F. Feng, W. Liu, Y. Chen, H. Sun, Highly potent and selective butyrylcholinesterase inhibitors for cognitive improvement and neuroprotection, J. Med. Chem. 64 (2021) 6856–6876, https://doi.org/10.1021/acs.jmedchem.1c00167.
[49] A.K. Sahoo, J. Dandapat, U.C. Dash, S. Kanhar, Features and outcomes of drugs for combination therapy as multi-targets strategy to combat Alzheimer's disease, J. Ethnopharmacol. 215 (2018) 42–73, https://doi.org/10.1016/j.jep.2017.12.015.
[50] A.M. Fanni, C.M. Vander Zanden, P.V. Majewska, J. Majewski, E.Y. Chi, Membrane-mediated fibrillation and toxicity of the tau hexapeptide PHF6, J. Biol. Chem. 294 (2019) 15304–15317, https://doi.org/10.1074/jbc.RA119.010003.
[51] M. Campora, C. Canale, E. Gatta, B. Tasso, E. Laurini, A. Relini, S. Pricl, M. Catto, M. Tonelli, Multitarget biological profiling of new naphthoquinone and anthraquinone-based derivatives for the treatment of alzheimer's disease, ACS Chem. Neurosci. 12 (2021) 447–461, https://doi.org/10.1021/acschemneuro.0c00624.
[52] R. Purgatorio, N. Gambacorta, M. Catto, M. de Candia, L. Pisani, A. Espargaró, R. Sabaté, S. Cellamare, O. Nicolotti, C.D. Altomare, Pharmacophore modeling and 3D-QSAR study of indole and isatin derivatives as antiamyloidogenic agents targeting alzheimer's disease, Molecules 25 (2020) E5773, https://doi.org/10.3390/molecules25235773.
[53] A. Sparatore, M. Veronese, F. Sparatore, [Quinolizidine derivatives with antimicrobial activity], Farm. Sci. 42 (1987) 159–174, https://doi.org/10.1002/chin.198745342.
[54] C. Boido Canu, G. Iusco, V. Boido, F. Sparatore, A. Sparatore, Synthesis and antileukemic activity of 1-[(quinolizidinylalkyl)amino]4/7-R-thioxanthen-9-ones, Farmaco 44 (1989) 1069–1082.
[55] M. Tonelli, A. Sparatore, N. Basilico, L. Cavicchini, S. Parapini, B. Tasso, E. Laurini, S. Pricl, V. Boido, F. Sparatore, Quinolizidine-derived lucanthone and amitriptyline analogues endowed with potent antileishmanial activity, Pharmaceuticals 13 (2020) E339, https://doi.org/10.3390/ph13110339.
[56] S. Archer, C.M. Suter, The preparation of some 1-alkylamino- and Dialkylaminoalkylaminothiaxanthones1, J. Am. Chem. Soc. 74 (1952) 4296–4309, https://doi.org/10.1021/ja01137a017.
[57] S. Archer, K.J. Miller, R. Rej, C. Periana, L. Fricker, Ring-hydroxylated analogues of lucanthone as antitumor agents, J. Med. Chem. 25 (1982) 220–227, https://doi.org/10.1021/jm00345a006.
[58] I. Bolognino, N. Giangregorio, L. Pisani, M. de Candia, R. Purgatorio, A. Tonazzi, C. D. Altomare, S. Cellamare, M. Catto, A prospective repurposing of dantrolene as a multitarget agent for alzheimer's disease, Molecules 24 (2019) E4298, https://doi.org/10.3390/molecules24234298.
[59] C. Dammers, D. Yolcu, L. Kukuk, D. Willbold, M. Pickhardt, E. Mandelkow, A.H. C. Horn, H. Sticht, M.N. Malhis, N. Will, J. Schuster, S.A. Funke, Selection and characterization of tau binding D-enantiomeric peptides with potential for therapy of alzheimer disease, PLoS One 11 (2016), e0167432, https://doi.org/10.1371/journal.pone.0167432.
[60] A. Espargaró, A. Medina, O. Di Pietro, D. Muñoz-Torrero, R. Sabate, Ultra rapid in vivo screening for anti-Alzheimer anti-amyloid drugs, Sci. Rep. 6 (2016), 23349, https://doi.org/10.1038/srep23349.
[61] S.L. Griner, P. Seidler, J. Bowler, K.A. Murray, T.P. Yang, S. Sahay, M.R. Sawaya, D. Cascio, J.A. Rodriguez, S. Philipp, J. Sosna, C.G. Glabe, T. Gonen, D. S. Eisenberg, Structure-based inhibitors of amyloid beta core suggest a common interface with tau, Elife 8 (2019), e46924, https://doi.org/10.7554/eLife.46924.
[62] M. Boban, M. Babić Leko, T. Miškić, P.R. Hof, G. Šimić, Human neuroblastoma SH-SY5Y cells treated with okadaic acid express phosphorylated high molecular weight tau-immunoreactive protein species, J. Neurosci. Methods 319 (2019) 60–68, https://doi.org/10.1016/j.jneumeth.2018.09.030.
[63] S. Sharma, N. Anand, in: S. Sharma, N. Anand (Eds.), Chapter 12 - Miscellaneous Anthelmintics, Pharmacochemistry Library, Elsevier, 1997, pp. 296–324, https://doi.org/10.1016/S0165-7208(97)80034-7.
[64] S. Zhou, G. Huang, The biological activities of butyrylcholinesterase inhibitors, Biomed. Pharmacother. 146 (2022), 112556, https://doi.org/10.1016/j.biopha.2021.112556.
[65] M. Hoffmann, C. Stiller, E. Endres, M. Scheiner, S. Gunesch, C. Sotriffer, T. Maurice, M. Decker, Highly selective butyrylcholinesterase inhibitors with tunable duration of action by chemical modification of transferable carbamate units exhibit pronounced neuroprotective effect in an alzheimer's disease mouse model, J. Med. Chem. 62 (2019) 9116–9140, https://doi.org/10.1021/acs.jmedchem.9b01012.
[66] L. Pisani, A. De Palma, N. Giangregorio, D.V. Miniero, P. Pesce, O. Nicolotti, F. Campagna, C.D. Altomare, M. Catto, Mannich base approach to 5-methoxyisatin 3-(4-isopropylphenyl)hydrazone: a water-soluble prodrug for a multitarget inhibition of cholinesterases, beta-amyloid fibrillization and oligomer-induced cytotoxicity, Eur. J. Pharmaceut. Sci. 109 (2017) 381–388, https://doi.org/10.1016/j.ejps.2017.08.004.
[67] M. Enguita, N. DeGregorio-Rocasolano, A. Abad, R. Trullas, Glycogen synthase kinase 3 activity mediates neuronal pentraxin 1 expression and cell death induced by potassium deprivation in cerebellar granule cells, Mol. Pharmacol. 67 (2005) 1237–1246, https://doi.org/10.1124/mol.104.007062.
[68] S. Vilches, C. Vergara, O. Nicolás, G. Sanclimens, S. Merino, S. Varón, G.A. Acosta, F. Albericio, M. Royo, J.A. Del Río, R. Gavín, Neurotoxicity of prion peptides mimicking the central domain of the cellular prion protein, PLoS One 8 (2013), e70881, https://doi.org/10.1371/journal.pone.0070881.
[69] D.A. Case, H.M. Aktulga, K. Belfon, I.Y. Ben-Shalom, J.T. Berryman, S.R. Brozell, D. S. Cerutti, T.E. Cheatham III, G.A. Cisneros, V.W.D. Cruzeiro, T.A. Darden, R. E. Duke, G. Giambasu, M.K. Gilson, H. Gohlke, A.W. Goetz, R. Harris, S. Izadi, S. A. Izmailov, K. Kasavajhala, M.C. Kaymak, E. King, A. Kovalenko, T. Kurtzman, T. S. Lee, S. LeGrand, P. Li, C. Lin, J. Liu, T. Luchko, R. Luo, M. Machado, V. Man, M. Manathunga, K.M. Merz, Y. Miao, O. Mikhailovskii, G. Monard, H. Nguyen, K. A. O'Hearn, A. Onufriev, F. Pan, S. Pantano, R. Qi, A. Rahnamoun, D.R. Roe, A. Roitberg, C. Sagui, S. Schott-Verdugo, A. Shajan, J. Shen, C.L. Simmerling, N. R. Skrynnikov, J. Smith, J. Swails, R.C. Walker, J. Wang, J. Wang, H. Wei, R. M. Wolf, X. Wu, Y. Xiong, Y. Xue, D.M. York, S. Zhao, P.A. Kollman, Amber 2022, University of California, San Francisco, 2022 (n.d.).
[70] E.F. Pettersen, T.D. Goddard, C.C. Huang, G.S. Couch, D.M. Greenblatt, E.C. Meng, T.E. Ferrin, UCSF Chimera–a visualization system for exploratory research and analysis, J. Comput. Chem. 25 (2004) 1605–1612, https://doi.org/10.1002/jcc.20084.
[71] Y. Nicolet, O. Lockridge, P. Masson, J.C. Fontecilla-Camps, F. Nachon, Crystal structure of human butyrylcholinesterase and of its complexes with substrate and products, J. Biol. Chem. 278 (2003) 41141–41147, https://doi.org/10.1074/jbc.M210241200.
[72] M. Estrada Valencia, C. Herrera-Arozamena, L. de Andrés, C. Pérez, J.A. Morales-García, A. Pérez-Castillo, E. Ramos, A. Romero, D. Viña, M. Yáñez, E. Laurini, S. Pricl, M.I. Rodríguez-Franco, Neurogenic and neuroprotective donepezil-flavonoid hybrids with sigma-1 affinity and inhibition of key enzymes in Alzheimer's disease, Eur. J. Med. Chem. 156 (2018) 534–553, https://doi.org/10.1016/j.ejmech.2018.07.026.
[73] M. Estrada, C. Pérez, E. Soriano, E. Laurini, M. Romano, S. Pricl, J.A. Morales-García, A. Pérez-Castillo, M.I. Rodríguez-Franco, New neurogenic lipoic-based hybrids as innovative Alzheimer's drugs with σ-1 agonism and β-secretase inhibition, Future Med. Chem. 8 (2016) 1191–1207, https://doi.org/10.4155/fmc-2016-0036.
[74] G.M. Morris, R. Huey, W. Lindstrom, M.F. Sanner, R.K. Belew, D.S. Goodsell, A. J. Olson, AutoDock 4 and AutoDockTools 4: automated docking with selective receptor flexibility, J. Comput. Chem. 30 (2009) 2785–2791, https://doi.org/10.1002/jcc.21256.

[75] W.L. Jorgensen, J. Chandrasekhar, J.D. Madura, R.W. Impey, M.L. Klein, Comparison of simple potential functions for simulating liquid water, J. Chem. Phys. 79 (1983) 926–935, https://doi.org/10.1063/1.445869.
[76] I. Massova, P.A. Kollman, Combined molecular mechanical and continuum solvent approach (MM-PBSA/GBSA) to predict ligand binding, Perspect. Drug Discov. Des. 18 (2000) 113–135, https://doi.org/10.1023/A:1008763014207.
[77] A. Onufriev, D. Bashford, D.A. Case, Modification of the generalized born model suitable for macromolecules, J. Phys. Chem. B 104 (2000) 3712–3720, https://doi.org/10.1021/jp994072s.